PROCEEDINGS OF SCIENCE

Associated production of H, W, Z with a $t\bar{t}$ pair at the LHC: theoretical predictions

Anna Kulesza*
Institute for Theoretical Physics, WWU Münster, D-48149 Münster, Germany
E-mail: anna.kulesza@uni-muenster.de

Leszek Motyka
Institute of Physics, Jagellonian University, S.Łojasiewicza 11, 30-348 Kraków, Poland
E-mail: leszekm@th.if.uj.edu.pl

Daniel Schwartländer
Institute for Theoretical Physics, WWU Münster, D-48149 Münster, Germany
E-mail: d_schw20@uni-muenster.de

Tomasz Stebel
Institute of Nuclear Physics PAN, Radzikowskiego 152, 31-342 Kraków, Poland
E-mail: tomasz.stebel@uj.edu.pl

Vincent Theeuwes
Institute for Theoretical Physics, Georg-August-Univesity Göttingen, Friedrich-Hund-Platz 1, 37077 Göttingen, Germany
E-mail: vincent.theeuwes@uni-goettingen.de

In this talk we review the status of the theoretical prediction for the associate production of top-antitop quark pairs with a heavy boson (Higgs, W,Z) at the LHC. In particular, we focus on recent calculations of the resummed cross sections for these processes at the next-to-next-leading logarithmic accuracy in direct QCD.

Corfu Summer Institute 2018 "School and Workshops on Elementary Particle Physics and Gravity" (CORFU2018)
31 August - 28 September, 2018
Corfu, Greece

*Speaker.

PoS(CORFU2018)024

The measurements [1, 2, 3, 4, 5, 6, 7, 8, 9, 10] of associated production of a heavy boson (H,W, Z) with a top-antitop quark pair provide an important test for the Standard Model at the LHC. These are the key processes to experimentally determine the top quark couplings. In particular, the associated $t\bar{t}H$ production directly probes the top Yukawa coupling without making any assumptions on its nature. Furthermore they are relevant in searches for new physics due to both being directly sensitive to it and providing an important background. The $t\bar{t}W$, $t\bar{t}Z$ processes also play an important role as a background for the associated Higgs boson production process $pp \to t\bar{t}H$. Thus it is necessary to know the theoretical predictions for $pp \to t\bar{t}B$, $B = H,W^{\pm},Z$ with high accuracy, especially in the light of ever improving precision of cross section measurements. For example, the very recent measurement of the $t\bar{t}Z$ cross section [10] carries statitical and systematic errors of only 5-7%.

Fixed order cross sections up to next-to-leading order in α_S are already known for some time both for the asociated Higgs boson[11, 12] and W and Z boson production [13, 14]. They were recalculated and matched to parton showers in [15, 16, 17, 18, 19, 20, 21, 22, 23]. Furthermore QCD-EW NLO corrections are also known [24, 25, 26]. For the $t\bar{t}H$ process, the NLO EW and QCD corrections to production with off-shell top quarks were also obtained [27, 28]. While NNLO calculations for this particular type of 2 to 3 processes are currently out of reach, a class of corrections beyond NLO from the emission of soft and/or collinear gluons can be taken into account with the help of resummation methods. Such methods allow to account for effects of soft gluon emission to all orders in perturbation theory. Two common approaches to perform soft gluon resummation are either calculations directly in QCD or in an effective field theory, in this case soft-collinear effective theory (SCET).

For the associated $t\bar{t}H$ production, the first calculations of the resummed cross section at the next-to-leading logarithmic (NLL) acuracy, matched to the NLO result were presented in [29]. The calculation relied on application of the traditional Mellin-space resummation formalism in the absolute threshold limit, i.e. in the limit of the partonic energy $\sqrt{\hat{s}}$ approaching the production threshold $M = 2m_t + m_H$. Subsequently, resummation of NLL corrections arising in the limit of $\sqrt{\hat{s}}$ approaching the invariant mass threshold Q, with $Q^2 = (p_t + p_{\bar{t}} + p_H)^2$, was performed in [30] and later extended to the next-to-next-to-leading-logarithmic (NNLL) accuracy and applied to the $t\bar{t}H$ production [31], as well as $t\bar{t}Z$ and $t\bar{t}W$ production [32]. Calculations in the framework of the soft-collinear effective theory (SCET) for the $t\bar{t}H$ process led first to obtaining approximate NNLO [33] and later full NNLL [34] predictions. NNLL+NLO predictions have been obtained in SCET for $pp \to t\bar{t}W$ [35, 36] and for $pp \to t\bar{t}Z$ in [37].

In the following we review results for threshold-resummed cross sections $pp \to t\bar{t}B$, $B = H,W,Z$ in the invariant mass kinematics, obtained using the Mellin-space approach at NNLL accuracy [31, 32].

1. Analytical description

In the following we treat the soft gluon corrections in the invariant mass kinematics, i.e we consider the limit $\hat{\rho} = \frac{Q^2}{\hat{s}} \to 1$ with $Q^2 = (p_t + p_{\bar{t}} + p_B)^2$. The logarithms resummed in the invariant

mass threshold limit have the form

$$\alpha_S^m \left(\frac{\log^n (1-\hat{\rho})}{1-\hat{\rho}} \right)_+ \qquad m \leq 2n-1 \tag{1.1}$$

with the plus distribution $\int_0^1 \mathrm{d}x (f(x))_+ = \int_0^1 \mathrm{d}x (f(x) - f(x_0))$. The Mellin moments of the differential cross section $\frac{\mathrm{d}\sigma_{ij\to t\bar{t}B}}{\mathrm{d}Q^2}$ are taken with respect to the variable $\rho = \frac{Q^2}{S}$. At the partonic level this leads to

$$\frac{\mathrm{d}\tilde{\hat{\sigma}}_{ij\to t\bar{t}B}}{\mathrm{d}Q^2}(N, Q^2, m_t, m_{W/Z}, \mu_R^2, \mu_F^2) = \int_0^1 \mathrm{d}\hat{\rho}\, \hat{\rho}^{N-1} \frac{\mathrm{d}\hat{\sigma}_{ij\to t\bar{t}B}}{\mathrm{d}Q^2}(\hat{\rho}, Q^2, m_t, m_{W/Z}, \mu_R^2, \mu_F^2) \tag{1.2}$$

for the Mellin moments for the process $ij \to t\bar{t}B$ with i,j denoting two massless colored partons. In Mellin space the threshold limit $\hat{\rho} \to 1$ corresponds to the limit $N \to \infty$. Since the process involves more than three colored partons, the resummed cross section is expressed in terms of color matrices. In Mellin space the resummed partonic cross section has the form [38, 39]

$$\frac{\mathrm{d}\tilde{\hat{\sigma}}_{ij\to t\bar{t}B}}{\mathrm{d}Q^2} = \mathrm{Tr}[\mathbf{H}_{ij\to t\bar{t}B} \mathbf{S}_{ij\to t\bar{t}B}] \Delta_i \Delta_j, \tag{1.3}$$

where $\mathbf{H}_{ij\to t\bar{t}W/Z}$ and $\mathbf{S}_{ij\to t\bar{t}B}$ are color matrices and the trace is taken in color space. We describe the evolution of color in the s-channel color basis, for which the basis vectors are

$$c_{\mathbf{1}} = \delta_{a_i,a_j}\delta_{a_k,a_l} \quad c_{\mathbf{8}} = T^c_{a_i,a_j} T^c_{a_k,a_l} \tag{1.4}$$

for the $q\bar{q}$ initial state and

$$c_{\mathbf{1}} = \delta_{a_i,a_j}\delta_{a_k,a_l} \quad c_{\mathbf{8S}} = d^{c,a_i,a_j} T^c_{a_k,a_l} \quad c_{\mathbf{8A}} = f^{c,a_i,a_j} T^c_{a_k,a_l} \tag{1.5}$$

for the gg initial state. This choice of color basis leads to a diagonal soft anomalous dimension matrix in the absolute threshold limit $\frac{(2m_t+m_B)^2}{\hat{s}} \to 1$, which is a special case of the invariant mass threshold limit. $\mathbf{H}_{ij\to t\bar{t}B}$ describes the hard scattering contributions projected on the color basis, while $\mathbf{S}_{ij\to t\bar{t}B}$ represents the soft wide angle emission. The (soft-)collinear logarithmic contributions form the initial state partons are taken into account by the functions Δ_i and Δ_j. They have been known for a long time [40, 41] and depend only on the emitting parton.

The soft function is given by a solution of the renormalization group equation [42, 43]:

$$\mathbf{S}_{ij\to klB}(N, Q^2, \mu_\mathrm{F}^2, \mu_\mathrm{R}^2) = \bar{\mathbf{U}}_{ij\to klB}(N, Q^2, \mu_\mathrm{F}^2, \mu_\mathrm{R}^2)\, \tilde{\mathbf{S}}_{ij\to klB}(\alpha_\mathrm{s}(Q^2/\bar{N}^2)) \mathbf{U}_{ij\to klB}(N, Q^2, \mu_\mathrm{F}^2, \mu_\mathrm{R}^2), \tag{1.6}$$

where $\tilde{\mathbf{S}}_{ij\to klB}$ plays a role of a boundary condition. This soft matrix, as well as the hard function $\mathbf{H}_{ij\to t\bar{t}B}$ can be calculated perturbatively [42, 44]:

$$\tilde{\mathbf{S}}_{ij\to klB} = \tilde{\mathbf{S}}^{(0)}_{ij\to klB} + \frac{\alpha_\mathrm{s}}{\pi} \tilde{\mathbf{S}}^{(1)}_{ij\to klB} + \ldots \qquad \mathbf{H}_{ij\to klB} = \mathbf{H}^{(0)}_{ij\to klB} + \frac{\alpha_\mathrm{s}}{\pi} \mathbf{H}^{(1)}_{ij\to klB} + \ldots$$

At the NNLL accuracy knowledge of $\tilde{\mathbf{S}}^{(1)}_{ij\to klB}$ and $\mathbf{H}^{(1)}_{ij\to klB}$ is required whereas for NLL only leading terms $\mathbf{H}^{(0)}_{ij\to klB}$, $\tilde{\mathbf{S}}^{(0)}_{ij\to klB}$ are needed.

The soft function evolution matrices $\mathbf{U}_{ij\to klB}$ are defined as a path-ordered exponents

$$\mathbf{U}_{ij\to klB}\left(N,Q^2,\mu_{\rm F}^2,\mu_{\rm R}^2\right)=\mathrm{P}\exp\left[\int_{\mu_{\rm F}}^{Q/\bar{N}}\frac{dq}{q}\mathbf{\Gamma}_{ij\to klB}\left(\alpha_{\rm s}\left(q^2\right)\right)\right], \tag{1.7}$$

where the soft anomalous dimension is calculated [29, 45] as a perturbative function in $\alpha_{\rm s}$,

$$\mathbf{\Gamma}_{ij\to klB}\left(\alpha_{\rm s}\right)=\left(\frac{\alpha_{\rm s}}{\pi}\right)\mathbf{\Gamma}^{(1)}_{ij\to klB}+\left(\frac{\alpha_{\rm s}}{\pi}\right)^2\mathbf{\Gamma}^{(2)}_{ij\to klB}+\ldots \tag{1.8}$$

In order to diagonalize the one-loop soft anomalous dimension matrix we make use of the transformation [47]:

$$\mathbf{\Gamma}^{(1)}_{R}=\mathbf{R}^{-1}\mathbf{\Gamma}^{(1)}_{ij\to klB}\mathbf{R}. \tag{1.9}$$

At NLL accuracy the evolution of the soft matrix $\mathbf{S}_{ij\to t\bar{t}B}$ is given by the one-loop anomalous dimension matrix, see e.g. [29]. By changing the colour basis to R-basis, the path ordered exponentials in Eq. (1.7), considered at NLL, reduce to simple exponentials given in terms of the eigenvalues $\lambda_I^{(1)}$ of the soft anomalous dimension matrix $\mathbf{\Gamma}^{(1)}_R$. Together with the LO contributions to the hard and soft function, this results in the following expression for the NLL cross section in the Mellin space

$$\begin{aligned}\frac{d\tilde{\hat{\sigma}}^{(\rm NLL)}_{ij\to klB}}{dQ^2}(N,Q^2,\{m^2\},\mu_{\rm F}^2,\mu_{\rm R}^2)\;=\;&\mathbf{H}^{(0)}_{R,IJ}(Q^2,\{m^2\})\,\tilde{\mathbf{S}}^{(0)}_{R,JI}\,\Delta^i(N+1,Q^2,\mu_{\rm F}^2,\mu_{\rm R}^2)\Delta^j(N+1,Q^2,\mu_{\rm F}^2,\mu_{\rm R}^2)\\ &\times\;\exp\left[\frac{\log(1-2\lambda)}{2\pi b_0}\left(\left(\lambda_J^{(1)}\right)^*+\lambda_I^{(1)}\right)\right],\end{aligned} \tag{1.10}$$

where the color indices I and J are implicitly summed over. The trace of the product of two matrices $\mathbf{H_R}^{(0)}$ and $\tilde{\mathbf{S}}^{(0)}_R$ returns the LO cross section. The incoming parton radiative factors Δ_i are now considered only at NLL accuracy.

In order to improve the accuracy of the numerical approximation provided by resummation, it is customary to include terms up to $\mathscr{O}(\alpha_{\rm s})$ in the expansion of the hard and soft function leading to

$$\begin{aligned}\frac{d\tilde{\hat{\sigma}}^{(\rm NLL\ w\ \mathscr{C})}_{ij\to klB}}{dQ^2}\;(N,Q^2,\{m^2\},\mu_{\rm F}^2,\mu_{\rm R}^2)&=\mathbf{H}_{R,IJ}(Q^2,\{m^2\},\mu_{\rm F}^2,\mu_{\rm R}^2)\,\tilde{\mathbf{S}}_{R,JI}(Q^2,\{m^2\})\\ \times\,\Delta^i(N+1,Q^2,\mu_{\rm F}^2,\mu_{\rm R}^2)\Delta^j(N+1,Q^2,\mu_{\rm F}^2,\mu_{\rm R}^2)&\exp\left[\frac{\log(1-2\lambda)}{2\pi b_0}\left(\left(\lambda_J^{(1)}\right)^*+\lambda_I^{(1)}\right)\right],\end{aligned} \tag{1.11}$$

where

$$\mathbf{H}_R\tilde{\mathbf{S}}_R=\mathbf{H}^{(0)}_R\tilde{\mathbf{S}}^{(0)}_R+\frac{\alpha_{\rm s}}{\pi}\left[\mathbf{H}^{(1)}_R\tilde{\mathbf{S}}^{(0)}_R+\mathbf{H}^{(0)}_R\tilde{\mathbf{S}}^{(1)}_R\right].$$

We will refer to this result as "NLL w $\mathscr{C}$", since the N-independent $\mathscr{O}(\alpha_{\rm s})$ terms in the hard and soft function are often collected together in one function, known as the hard matching coefficient, $\mathscr{C}$. Although we choose to treat these terms as in Eq. (1.12), we keep the name "w $\mathscr{C}$" ("w" standing for "with") as a useful shorthand. The virtual contributions which enter $\mathbf{H}^{(1)}_R$ are extracted from the `PowHel` code [17, 19, 23, 22] and projected on the colour basis. The extraction of the virtual contributions has been checked with `MadGraph5_aMC@NLO` [21].

In NNLL calculations, other matrices are also transformed using diagonalization matrix $\mathbf{R}$:

$$\mathbf{\Gamma}^{(2)}_R=\mathbf{R}^{-1}\mathbf{\Gamma}^{(2)}_{ij\to klB}\mathbf{R},\qquad \mathbf{H}_R=\mathbf{R}^{-1}\mathbf{H}_{ij\to klB}\left(\mathbf{R}^{-1}\right)^\dagger,\qquad \tilde{\mathbf{S}}_R=\mathbf{R}^\dagger\tilde{\mathbf{S}}_{ij\to klB}\mathbf{R}.$$

In the **R**-representation the evolution factor $\mathbf{U}_R$ (similarly $\bar{\mathbf{U}}_R$) can be written at NNLL accuracy as [48, 49]:

$$\mathbf{U}_R(N,Q^2,Q^2,\mu_{\rm R}^2) = \left(\mathbf{1}+\frac{\alpha_{\rm s}(\mu_{\rm R}^2)}{\pi[1-2\alpha_{\rm s}(\mu_{\rm R}^2)b_0\log N]}\mathbf{K}\right)\left[e^{g_s(N)\vec{\lambda}^{(1)}}\right]_D\left(\mathbf{1}-\frac{\alpha_{\rm s}(\mu_{\rm R}^2)}{\pi}\mathbf{K}\right), \quad (1.12)$$

where $K_{IJ} = \delta_{IJ}\lambda_I^{(1)}\frac{b_1}{2b_0^2} - \frac{\left(\mathbf{\Gamma}_R^{(2)}\right)_{IJ}}{2\pi b_0+\lambda_I^{(1)}-\lambda_J^{(1)}}$. By $\left[e^{g_s(N)\vec{\lambda}^{(1)}}\right]_D$ we have denoted diagonal matrix with exponentiated eigenvalues on diagonal and $g_s(N)$ is a function which resumms logarithms of N (see [31] for expression), b_0 and b_1 are the first two coefficients of expansion $\beta_{\rm QCD}$ in $\alpha_{\rm s}$.

2. Numerical results

The numerical results were obtained using the same set up for input parameters as the one used in the HXSWG Yellow Report 4 [50]. In particular, we use $m_t = 172.5\,\text{GeV}$, $m_H = 125\,\text{GeV}$, $m_W = 80.385\,\text{GeV}$, $m_Z = 91.188\,\text{GeV}$, $G_F = 1.1663787\times10^{-5}\ \text{GeV}^{-2}$ and the PDF4LHC15_30 parton distribution function sets [51, 52, 53, 54, 55, 56] with the corresponding values of $\alpha_{\rm s}$. The NLO sets are employed for the NLO+NLL predictions, whereas the NLO+NNLL predictions are calculated with NNLO sets. The NLO cross section is obtained using the `MadGraph5_aMC@NLO` code [21].

In Table **??** we show our numerical predictions for the total cross sections at 13 TeV with three choices of the central value of the renormalization and factorization scales: $\mu_0 = \mu_{\rm F,0} = \mu_{\rm R,0} = Q$, $\mu_0 = \mu_{\rm F,0} = \mu_{\rm R,0} = M/2 = m_t + m_B/2$ ($B = H,W,Z$) and the 'in-between' value of $\mu_0 = \mu_{\rm F,0} = \mu_{\rm R,0} = Q/2$. By studying results for these relatively distant scales, we aim to cover a span of scale choices relevant in the problem. The theoretical error due to scale variation is calculated using the so called 7-point method, where the minimum and maximum values obtained with $(\mu_{\rm F}/\mu_0, \mu_{\rm R}/\mu_0) = (0.5,0.5),(0.5,1),(1,0.5),(1,1),(1,2),(2,1),(2,2)$ are considered. Total cross section results were obtained by integrating the resummed differential cross section $\frac{{\rm d}\tilde{\sigma}}{{\rm d}Q^2}$. The resummed results are then matched [31] to fixed order NLO predictions. The results presented in Table **??** are illustrated in Fig. 1.

The NLO values listed here fully agree with the NLO QCD cross sections published in the HXSWG Yellow Report 4 [50] within statistical Monte Carlo errors. Although the NLO results for various scale choices span quite a large range of values, we observe the results get closer as the accuracy of resummation improves from NLL to NNLL, indicating the importance of resummed calculations. Another manifestation of the same effect originating from soft gluon corrections is the decrease in the scale uncertainties calculated for each specific scale choice which is also progressing with increasing precision of the theoretical predictions. These trends are much stronger for $t\bar{t}H$ and $t\bar{t}Z$ production than for $t\bar{t}W$ due to the gg channel contributing to the LO and, correspondingly, to the resummed cross section. As the gluon radiate more than quarks, resummation has more relevance for the gg production channel than for $q\bar{q}$ or $q\bar{q}^{'}$ channels. In Table **??** we also list the $K_{\rm NNLL}$ factor measuring the impact of the higher-order logarithmic corrections, defined as the ratio of the NLO+NNLL to NLO cross sections. It varies depending on the value of the central scale. The variation is almost entirely driven by the scale dependence of the NLO cross section. For the choice $\mu_0 = Q$ the $K_{\rm NNLL}$-factor can be as high as 1.29 (1.19) for the $t\bar{t}Z$ ($t\bar{t}H$) cross section.

process	μ_0	NLO [fb]	NLO+NLL[fb]	NLO+NLL w $\mathscr{C}$ [fb]	NLO+NNLL[fb]	$K_{\rm NNLL}$
$t\bar{t}H$	Q	$418^{+12.2\%}_{-11.6\%}$	$439^{+10.1\%}_{-9.2\%}$	$484^{+8.4\%}_{-8.5\%}$	$499^{+7.6\%}_{-6.9\%}$	1.19
	$Q/2$	$469^{+9.6\%}_{-10.9\%}$	$478^{+8.4\%}_{-8.2\%}$	$497^{+5.9\%}_{-7.3\%}$	$498^{+6.0\%}_{-6.0\%}$	1.06
	$M/2$	$498^{+5.8\%}_{-9.1\%}$	$502^{+8.1\%}_{-7.6\%}$	$504^{+5.7\%}_{-5.8\%}$	$504^{+5.3\%}_{-6.0\%}$	1.01
$t\bar{t}Z$	Q	$659^{+14.1\%}_{-12.7\%}$	$696^{+11.7\%}_{-10.2\%}$	$795^{+10.8\%}_{-9.8\%}$	$848^{+8.3\%}_{-8.3\%}$	1.29
	$Q/2$	$752^{+12.7\%}_{-12.4\%}$	$770^{+10.8\%}_{-9.6\%}$	$825^{+8.9\%}_{-8.9\%}$	$856^{+7.2\%}_{-7.9\%}$	1.14
	$M/2$	$843^{+9.7\%}_{-11.3\%}$	$850^{+11.5\%}_{-9.8\%}$	$861^{+7.3\%}_{-7.9\%}$	$875^{+7.0\%}_{-7.7\%}$	1.04
$t\bar{t}W^+$	Q	$323^{+12.2\%}_{-10.8\%}$	$325^{+11.8\%}_{-10.4\%}$	$336^{+9.8\%}_{-9.2\%}$	$342^{+8.9\%}_{-8.6\%}$	1.06
	$Q/2$	$363^{+12.1\%}_{-10.9\%}$	$364^{+11.9\%}_{-10.6\%}$	$368^{+10.4\%}_{-9.1\%}$	$371^{+9.7\%}_{-8.7\%}$	1.02
	$M/2$	$413^{+12.7\%}_{-11.4\%}$	$414^{+13.1\%}_{-11.3\%}$	$413^{+13.0\%}_{-10.0\%}$	$415^{+12.9\%}_{-9.6\%}$	1.01
$t\bar{t}W^-$	Q	$163^{+12.5\%}_{-10.9\%}$	$165^{+12\%}_{-10.4\%}$	$171^{+9.9\%}_{-9.2\%}$	$176^{+8.8\%}_{-8.6\%}$	1.08
	$Q/2$	$184^{+12.4\%}_{-11.1\%}$	$185^{+12.1\%}_{-10.7\%}$	$187^{+10.4\%}_{-9.1\%}$	$191^{+9.6\%}_{-8.7\%}$	1.04
	$M/2$	$208^{+13.4\%}_{-11.6\%}$	$209^{+13.8\%}_{-11.4\%}$	$209^{+13.5\%}_{-9.9\%}$	$212^{+13.2\%}_{-9.5\%}$	1.02

Table 1: Total cross section predictions for $pp \to t\bar{t}B$, $B = H,Z,W^\pm$ at $\sqrt{S} = 13$ TeV and for various central scale choices and resummation accuracies. The listed error is the theoretical error due to scale variation calculated using the 7-point method.

Given the conspicuous stability of the NLO+NNLL results, see Fig. 1, we are encouraged to combine our results obtained for various scale choices. For this purpose we adopt the method proposed by the Higgs Cross Section Working Group [57]. In this way, we obtain at 13 TeV for the $t\bar{t}H$ cross section

$$\sigma^{t\bar{t}H}_{\rm NLO+NNLL} = 500^{+7.3\%+3.0\%}_{-7.1\%-3.0\%}\ {\rm fb}, \tag{2.1}$$

and

$$\sigma^{t\bar{t}Z}_{\rm NLO+NNLL} = 863^{+8.5\%+3.2\%}_{-9.9\%-3.2\%}\ {\rm fb}, \tag{2.2}$$

for the $t\bar{t}Z$ cross section, as well as

$$\sigma^{t\bar{t}W^+}_{\rm NLO+NNLL} = 374^{+25.3\%+3.2\%}_{-16.4\%-3.2\%}\ {\rm fb}, \tag{2.3}$$

$$\sigma^{t\bar{t}W^-}_{\rm NLO+NNLL} = 192^{+25.2\%+3.7\%}_{-16.1\%-3.7\%}\ {\rm fb}, \tag{2.4}$$

for the $t\bar{t}W^\pm$ cross sections. The first uncertainty originates from the scale variation and is calculated using the envelope method, whereas the second one is the pdf+$\alpha_{\rm s}$ uncertainty. The combined results above should be understood as theoretical predictions with a conservative estimate of the theory error. However, it needs to be stressed that even such conservative error estimate provides a considerable improvement of the scale error in comparison with the NLO results. In particular, for the $t\bar{t}Z$ production the overall size of the theory error at NLO+NNLL is comparable with overall experimental error of the latest CMS measurement [10], in contrast to the NLO predictions at the central scale $\mu_0 = \mu_{\rm F,0} = \mu_{\rm R,0} = M/2$, quoted by [10] and listed in Table **??**. If only the NLO+NNLL for the central scale choice $\mu_0 = \mu_{\rm F,0} = \mu_{\rm R,0} = M/2$ is considered, the scale error is smaller than in the combined case, see Table **??** and Eq. (2.2), amounting to 7-8%, and thus being comparable with the systematic error of the latest measurement [10].

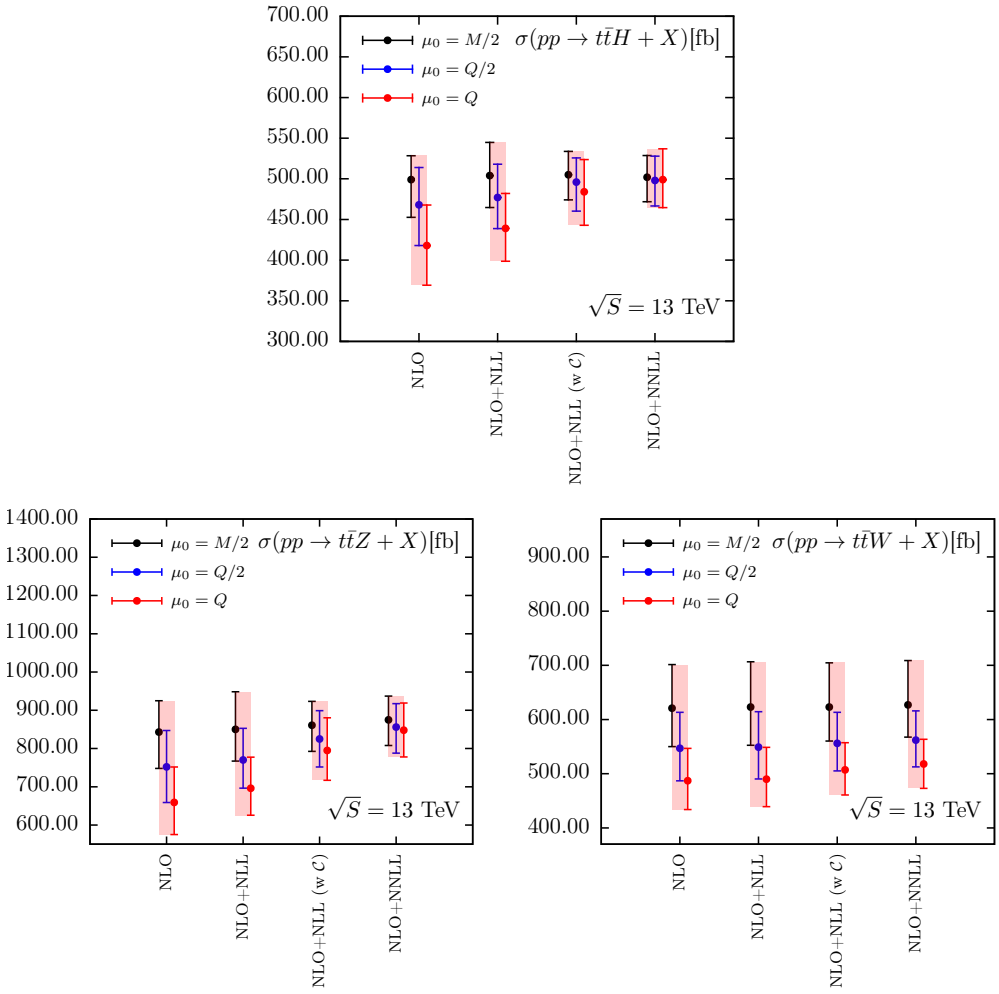

Figure 1: Graphical illustration of results presented in Table 1. The $t\bar{t}W^+$ and $t\bar{t}W^-$ in Table 1 are summed together.

Acknowledgments

This work has been supported in part by the DFG Grant KU 3103/1 and by Polish National Science Center (NCN) grant No. 2017/27/B/ST2/02755. TS would like to thank the Ministry of Science and Higher Education of Poland for support in the form of the Mobility Plus grant as well as Brookhaven National Laboratory for hospitality and support. The work leading to this publication was also supported by the German Academic Exchange Service (DAAD) with funds from the German Federal Ministry of Education and Research (BMBF) and the People Programme (Marie Curie Actions) of the European Union Seventh Framework Programme (FP7/2007-2013) under REA grant agreement n. 605728 (P.R.I.M.E. Postdoctoral Researchers International Mobility Experience).

References

[1] A. M. Sirunyan *et al.* [CMS Collaboration], Phys. Rev. Lett. **120** (2018) no.23, 231801 doi:10.1103/PhysRevLett.120.231801 [arXiv:1804.02610 [hep-ex]].

[2] M. Aaboud *et al.* [ATLAS Collaboration], Phys. Lett. B **784** (2018) 173 doi:10.1016/j.physletb.2018.07.035 [arXiv:1806.00425 [hep-ex]].

[3] S. Chatrchyan *et al.* [CMS Collaboration], Phys. Rev. Lett. **110** (2013) 172002 [arXiv:1303.3239 [hep-ex]].

[4] V. Khachatryan *et al.* [CMS Collaboration], Eur. Phys. J. C **74** (2014) no.9, 3060 [arXiv:1406.7830 [hep-ex]].

[5] G. Aad *et al.* [ATLAS Collaboration], JHEP **1511** (2015) 172 [arXiv:1509.05276 [hep-ex]].

[6] V. Khachatryan *et al.* [CMS Collaboration], JHEP **1601** (2016) 096 [arXiv:1510.01131 [hep-ex]].

[7] M. Aaboud *et al.* [ATLAS Collaboration], Eur. Phys. J. C **77** (2017) no.1, 40 [arXiv:1609.01599 [hep-ex]].

[8] A. M. Sirunyan *et al.* [CMS Collaboration], JHEP **1808** (2018) 011 [arXiv:1711.02547 [hep-ex]].

[9] M. Aaboud *et al.* [ATLAS Collaboration], arXiv:1901.03584 [hep-ex].

[10] CMS Collaboration [CMS Collaboration], CMS-PAS-TOP-18-009.

[11] W. Beenakker, S. Dittmaier, M. Krämer, B. Plumper, M. Spira and P. M. Zerwas, Phys. Rev. Lett. **87** (2001) 201805 [hep-ph/0107081]; W. Beenakker, S. Dittmaier, M. Krämer, B. Plumper, M. Spira and P. M. Zerwas, Nucl. Phys. B **653** (2003) 151 [hep-ph/0211352].

[12] L. Reina and S. Dawson, Phys. Rev. Lett. **87** (2001) 201804 [hep-ph/0107101]; L. Reina, S. Dawson and D. Wackeroth, Phys. Rev. D **65** (2002) 053017 [hep-ph/0109066]; S. Dawson, L. H. Orr, L. Reina and D. Wackeroth, Phys. Rev. D **67** (2003) 071503 [hep-ph/0211438]; S. Dawson, C. Jackson, L. H. Orr, L. Reina and D. Wackeroth, Phys. Rev. D **68** (2003) 034022 [hep-ph/0305087].

[13] A. Lazopoulos, T. McElmurry, K. Melnikov and F. Petriello, *Phys. Lett. B* **666** (2008) 62 [arXiv:0804.2220 [hep-ph]].

[14] A. Lazopoulos, K. Melnikov and F. J. Petriello, *Phys. Rev. D* **77** (2008) 034021 [arXiv:0709.4044 [hep-ph]].

[15] V. Hirschi, R. Frederix, S. Frixione, M. V. Garzelli, F. Maltoni and R. Pittau, JHEP **1105** (2011) 044 [arXiv:1103.0621 [hep-ph]].

[16] R. Frederix, S. Frixione, V. Hirschi, F. Maltoni, R. Pittau and P. Torrielli, Phys. Lett. B **701** (2011) 427 [arXiv:1104.5613 [hep-ph]].

[17] M. V. Garzelli, A. Kardos, C. G. Papadopoulos and Z. Trocsanyi, Europhys. Lett. **96** (2011) 11001 [arXiv:1108.0387 [hep-ph]].

[18] H. B. Hartanto, B. Jager, L. Reina and D. Wackeroth, Phys. Rev. D **91** (2015) 9, 094003 [arXiv:1501.04498 [hep-ph]].

[19] A. Kardos, Z. Trocsanyi and C. Papadopoulos, *Phys. Rev. D* **85** (2012) 054015 [arXiv:1111.0610 [hep-ph]].

[20] J. M. Campbell and R. K. Ellis, *JHEP* **1207** (2012) 052 [arXiv:1204.5678 [hep-ph]].

[21] J. Alwall *et al.*, *JHEP* **1407** (2014) 079 [arXiv:1405.0301 [hep-ph]].

[22] M. V. Garzelli, A. Kardos, C. G. Papadopoulos and Z. Trocsanyi, *Phys. Rev. D* **85** (2012) 074022 [arXiv:1111.1444 [hep-ph]].

[23] M. V. Garzelli, A. Kardos, C. G. Papadopoulos and Z. Trocsanyi, *JHEP* **1211** (2012) 056 [arXiv:1208.2665 [hep-ph]].

[24] S. Frixione, V. Hirschi, D. Pagani, H. S. Shao and M. Zaro, JHEP **1409** (2014) 065 [arXiv:1407.0823 [hep-ph]].

[25] S. Frixione, V. Hirschi, D. Pagani, H.-S. Shao and M. Zaro, JHEP **1506** (2015) 184 [arXiv:1504.03446 [hep-ph]].

[26] Y. Zhang, W. G. Ma, R. Y. Zhang, C. Chen and L. Guo, Phys. Lett. B **738** (2014) 1 [arXiv:1407.1110 [hep-ph]].

[27] A. Denner and R. Feger, JHEP **1511** (2015) 209 [arXiv:1506.07448 [hep-ph]].

[28] A. Denner, J. N. Lang, M. Pellen and S. Uccirati, JHEP **1702** (2017) 053 [arXiv:1612.07138 [hep-ph]].

[29] A. Kulesza, L. Motyka, T. Stebel and V. Theeuwes, *JHEP* 1603 (2016) 065 [arXiv:1509.02780 [hep-ph]].

[30] A. Kulesza, L. Motyka, T. Stebel and V. Theeuwes, PoS LHCP **2016** (2016) 084 doi:10.22323/1.276.0084 [arXiv:1609.01619 [hep-ph]].

[31] A. Kulesza, L. Motyka, T. Stebel and V. Theeuwes, Phys. Rev. D **97** (2018) no.11, 114007 doi:10.1103/PhysRevD.97.114007 [arXiv:1704.03363 [hep-ph]].

[32] A. Kulesza, L. Motyka, D. Schwartländer, T. Stebel and V. Theeuwes, Eur. Phys. J. C **79** (2019) no.3, 249 doi:10.1140/epjc/s10052-019-6746-z [arXiv:1812.08622 [hep-ph]].

[33] A. Broggio, A. Ferroglia, B. D. Pecjak, A. Signer and L. L. Yang, JHEP **1603** (2016) 124 [arXiv:1510.01914 [hep-ph]].

[34] A. Broggio, A. Ferroglia, B. D. Pecjak and L. L. Yang, JHEP **1702** (2017) 126 [arXiv:1611.00049 [hep-ph]].

[35] H. T. Li, C. S. Li and S. A. Li, *Phys. Rev. D* **90** (2014) no.9, 094009 [arXiv:1409.1460 [hep-ph]].

[36] A. Broggio, A. Ferroglia, G. Ossola and B. D. Pecjak, *JHEP* **1609** (2016) 089 [arXiv:1607.05303 [hep-ph]].

[37] A. Broggio, A. Ferroglia, G. Ossola, B. D. Pecjak and R. D. Sameshima, *JHEP* **1704** (2017) 105 [arXiv:1702.00800 [hep-ph]].

[38] H. Contopanagos, E. Laenen and G. F. Sterman, *Nucl. Phys. B* **484** (1997) 303 [hep-ph/9604313].

[39] N. Kidonakis, G. Oderda and G. F. Sterman, *Nucl. Phys. B* **531** (1998) 365 [hep-ph/9803241].

[40] S. Catani, M. L. Mangano, P. Nason and L. Trentadue, *Nucl. Phys. B* **478** 273 (1996) [hep-ph/9604351].

[41] R. Bonciani, S. Catani, M. L. Mangano and P. Nason, *Nucl. Phys. B* **529** 424 (1998) [hep-ph/9801375].

[42] N. Kidonakis and G. Sterman, Nucl. Phys. B **505** (1997) 321 [arXiv:hep-ph/9705234].

[43]

[43] M. Czakon, A. Mitov and G. F. Sterman, Phys. Rev. D **80** (2009) 074017 [arXiv:0907.1790 [hep-ph]]. [44]

[44] L. J. Dixon, L. Magnea and G. F. Sterman, JHEP **0808** (2008) 022 [arXiv:0805.3515 [hep-ph]].

[45] A. Ferroglia, M. Neubert, B. D. Pecjak and L. L. Yang, Phys. Rev. Lett. **103** (2009) 201601 [arXiv:0907.4791 [hep-ph]].

[46] A. Ferroglia, M. Neubert, B. D. Pecjak and L. L. Yang, JHEP **0911** (2009) 062 [arXiv:0908.3676 [hep-ph]].

[47] N. Kidonakis, G. Oderda and G. Sterman, Nucl. Phys. B **525**, 299 (1998) [arXiv:hep-ph/9801268].

[48] A. J. Buras, Rev. Mod. Phys. **52** (1980) 199.

[49] V. Ahrens, A. Ferroglia, M. Neubert, B. D. Pecjak and L. L. Yang, JHEP **1009** (2010) 097 [arXiv:1003.5827 [hep-ph]].

[50] D. de Florian *et al.* [LHC Higgs Cross Section Working Group], arXiv:1610.07922 [hep-ph].

[51] J. Butterworth *et al.*, J. Phys. G **43** (2016) 023001 [arXiv:1510.03865 [hep-ph]].

[52] S. Dulat *et al.*, Phys. Rev. D **93** (2016) no.3, 033006 [arXiv:1506.07443 [hep-ph]].

[53] L. A. Harland-Lang, A. D. Martin, P. Motylinski and R. S. Thorne, Eur. Phys. J. C **75** (2015) no.5, 204 [arXiv:1412.3989 [hep-ph]].

[54] R. D. Ball *et al.* [NNPDF Collaboration], JHEP **1504** (2015) 040 [arXiv:1410.8849 [hep-ph]].

[55] J. Gao and P. Nadolsky, JHEP **1407** (2014) 035 [arXiv:1401.0013 [hep-ph]].

[56] S. Carrazza, S. Forte, Z. Kassabov, J. I. Latorre and J. Rojo, Eur. Phys. J. C **75** (2015) no.8, 369 [arXiv:1505.06736 [hep-ph]].

[57] S. Dittmaier *et al.* [LHC Higgs Cross Section Working Group Collaboration], arXiv:1101.0593 [hep-ph].